

The role of urea in Cu–Zn–Al catalysts for methanol steam reforming

Suparoek Henpraserttae · Pimpa Limthongkul ·
Pisanu Toochinda

Received: 6 August 2009 / Accepted: 20 January 2010 / Published online: 13 March 2010
© Springer-Verlag 2010

Abstract Impregnated Cu–Zn over Al₂O₃ exhibits high activity with the use of a lower amount of active metal relative to conventional co-precipitation catalysts. The activity of the catalyst could be enhanced by addition of urea to the metal salt solution during impregnation. The H₂ yield from Cu–Zn catalysts with urea is 42%, while the H₂ yield from catalyst without urea is only 28% in a continuous system at 250 °C and 1.2 atm. The H₂ yield of the catalyst with urea in this study could compete with that of commercial catalysts. The role of urea in the Cu–Zn catalysts was investigated. X-ray diffraction (XRD) analysis of the catalysts shows that the crystal size of CuO could be reduced by the addition of urea. The XRD diffractogram of the catalyst prior to calcination also shows the formation of NH₄NO₃, which could aid in dissociation of metal clusters. Scanning electron microscopy (SEM) images of catalysts show the size of Cu–Zn compound clusters and also their dispersion over the Al₂O₃ surface on the impregnated catalysts. The addition of urea could also yield smaller Cu–Zn compound clusters and better dispersion compared with

the impregnated catalyst without urea. Such impregnated Cu–Zn catalysts with urea could be alternative novel catalysts for methanol steam reforming.

Keywords Methanol steam reforming · Hydrogen production · Cu–Zn-based catalyst · Incipient wetness impregnation · Role of urea

Introduction

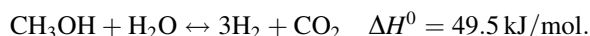
Hydrogen fuel cells are considered as one of the promising energy resources for replacement of fossil fuels. Unfortunately, gathering hydrogen resources is a major obstacle for the use of hydrogen fuel cells. Unlike oxygen, which is abundant in the atmosphere, hydrogen cannot be easily obtained from any resource without production processes. Hydrogen can be produced from dissociation of water or reforming reactions of hydrocarbons such as methane, ethanol, methanol, etc. [1, 4, 9]. Unfortunately, these hydrogen production processes require high energy expenditure to obtain effective hydrogen yields. The methane reforming reaction requires high reaction temperatures of 973–1,273 K [17, 19], while the reforming of alcohol requires lower reaction temperature [4, 6] to obtain equivalent hydrogen yield. One of the attractive hydrocarbons for hydrogen production by the reforming reaction is methanol. Methanol has a low boiling point and reforming temperature, a high energy density and H/C ratio, can be easily stored, and is available at low cost. Among the hydrogen production methods based on reforming reactions of methanol, the methanol steam reforming reaction exhibits the highest hydrogen yield with moderate energy consumption. The reaction is shown as follows [3, 11, 14].

S. Henpraserttae · P. Toochinda (✉)
School of Bio-Chemical Engineering and Technology,
Sirindhorn International Institute of Technology,
Thammasat University, P.O. Box 22,
Pathum Thani 12121, Thailand
e-mail: pisanu@siit.tu.ac.th

S. Henpraserttae
e-mail: suparoeh@mtec.or.th

P. Limthongkul
National Metal and Materials Technology Center,
National Science and Technology Development Agency,
Klong-1, Klong Luang, Pathum Thani 12120, Thailand

Methanol steam reforming:



Catalytic reforming reactions are generally operated at a temperature of 523–573 K to produce an effective hydrogen yield [11, 13, 18]. Most of the catalysts for the methanol steam reforming reaction are Cu–Zn-based catalysts, which are prepared by precipitation methods. Most Cu–Zn-based catalysts and commercial catalysts are prepared by using Cu and Zn contents as high as 60–90 wt% by the co-precipitation method to produce a high yield of hydrogen [11, 14]. Incipient wetness impregnation over high-surface-area materials has been widely used for the preparation of many catalysts to increase the number of active sites and the surface area, providing an easy method and the use of a small amount of active metal relative to other catalyst preparation methods, which can lower the costs of catalyst production [10]. The literature reports on the use of urea in precipitation of Cu–Zn-based catalysts to improve their activity for hydrogen production [5, 8, 13–16]. Unfortunately, the role of urea in precipitation of Cu–Zn catalysts remains unclear. Impregnation of Cu and Zn on an alumina support, integrated with the use of urea, might lead to the development of an effective catalyst preparation method for the methanol steam reforming reaction. Such a catalyst may exhibit high activity for hydrogen production without using high metal loading on the catalyst.

The objective of this work is to study the effect of urea addition in catalyst preparation by the impregnation method. The performance of the resulting catalysts is compared with the performance of a commercial catalyst made by a precipitation method. The role of urea in catalyst preparation by impregnation is also investigated. The results of this study may lead to better understanding of the role of urea in catalyst preparation for the development of effective catalysts for hydrogen production by the methanol reforming process.

Results and discussion

Activity of catalysts for methanol reforming

Table 1 reports the activity of various catalysts for hydrogen production by the methanol steam reforming reaction. H₂ yields were calculated using the following equation derived from the stoichiometric coefficients of methanol and hydrogen in the balanced chemical reaction:

$$\% \text{H}_2 \text{ yield} = \frac{1}{3} \frac{\text{mol of H}_2}{\text{mol of CH}_3\text{OH fed}} \times 100$$

Table 1 shows that a higher amount of metal loading leads to higher catalyst activity, as evidenced by the higher

Table 1 Hydrogen production from methanol reforming over various catalysts at 453 and 523 K

Cu–Zn–Al ₂ O ₃ catalysts (Cu/Zn/Al ₂ O ₃ (%wt))	H ₂ yield (%)
Temperature, 453 K	
10CZ (5/5/90)	<10
10CZU1 (5/5/90)	<10
10CZU2 (5/5/90)	14
20CZ (10/10/80)	13
20CZNa (10/10/80)	13
20CZU1 (10/10/80)	15
20CZU2 (10/10/80)	19
Commercial (40/30/30)	27
Temperature, 523 K	
10CZ (5/5/90)	14
10CZU1 (5/5/90)	20
10CZU2 (5/5/90)	23
20CZ (10/10/80)	28
20CZNa (10/10/80)	28
20CZU1 (10/10/80)	35
20CZU2 (10/10/80)	42
Commercial (40/30/30)	43

activity of the 20 wt% metal loading catalysts (20CZ, 20CZU1, 20CZU2) compared with those with 10 wt% metal loading (10CZ, 10CZU1, 10CZU2) at both 453 and 523 K. The data also show that the amount of urea affects the catalyst activity for both 10 and 20 wt% metal loading. CZU2 exhibits higher hydrogen yield than does CZU1 at both 453 and 523 K. The results show that use of a high amount of urea in catalyst preparation can enhance catalyst activity for hydrogen production. Table 1 also shows that 20CZU2 can exhibit high activity (42% H₂ yield), comparable to that of commercial catalyst (43% H₂ yield) at 523 K. The Cu and Zn loading of impregnated 20CZU2 (Cu/Zn/Al₂O₃: 10/10/80 wt%) is much lower than that of commercial precipitated catalyst (Cu/Zn/Al₂O₃: 40/30/30 wt%). Unlike the addition of urea, the data show that there is no improvement in catalyst activity with the addition of NaOH, which is also indicated by the fact that 20CZU1 and 20CZU2 exhibit higher activity than 20CZNa. The data show that the improvement of catalytic activity of CZU catalysts does not result from the basicity of the metal salt solution in the impregnation process. The role of urea in the improvement of catalyst activity for hydrogen production will be discussed in a later section.

Phase and morphology characterization

The CZ, CZU, CZNa, and commercial catalysts were characterized by scanning electron microscopy (SEM) with

energy-dispersive spectrometry (EDS) and X-ray diffraction (XRD) to inspect their physical characteristics, crystal size, and morphology, before and after calcination.

Figures 1 and 2 show SEM–EDS images of the CZ and CZU catalyst, respectively, after calcination. The images of these two types of catalysts show that Cu and Zn are deposited in the form of small clusters on the Al_2O_3 surface. The EDS profiles clearly indicate that the small clusters are composed of Cu and Zn located on Al_2O_3 . The SEM images also show that the sizes of the Cu–Zn clusters on the catalysts with urea (CZU) are much smaller than those of the catalysts without urea (CZ). The addition of urea can enable the formation of smaller Cu–Zn compound clusters.

Figure 3 shows an SEM–EDS image of the commercial catalyst. This image shows that Cu, Zn, and Al are mixed well throughout the entire catalyst without the formation of any separated metal clusters. The EDS profile shows that the catalyst surface is composed of Cu, Zn, and Al species all together.

Figure 4 shows SEM images of catalysts with and without urea at 20 wt% metal loading after calcination. The SEM images of 20CZ (Fig. 4a) show the agglomeration of large Cu–Zn compound clusters ($>10\ \mu\text{m}$) over Al_2O_3 . The distribution of Cu–Zn compound clusters is inconsistent over the Al_2O_3 surface. The SEM images of 20CZU1 (Fig. 4b) show smaller Cu–Zn compound clusters ($\approx 2\text{--}6\ \mu\text{m}$) and

better dispersion of Cu–Zn compound clusters over Al_2O_3 compared with 20CZ. The SEM images of 20CZU2 (Fig. 4c) clearly show the smallest Cu–Zn compound clusters ($\approx 0.2\text{--}1\ \mu\text{m}$) among the catalysts investigated in this study and also the best distribution of Cu–Zn compound clusters over the surface of Al_2O_3 . The images also show that the good dispersion of small Cu–Zn compound clusters on Al_2O_3 for 20CZU2 corresponds to the highest hydrogen yield for 20CZU2 among the impregnated Cu–Zn catalysts investigated in this study.

Figure 5 shows SEM images of CZ, CZU, and CZNa catalysts with 20 wt% metal loading before and after calcination. Figure 5a shows the crystal morphology of Cu–Zn compound clusters in the form of a rod-like structure before calcination. After calcination, the Cu–Zn compound clusters agglomerate to form large clusters over Al_2O_3 . Figure 5b shows the crystal morphology of the Cu–Zn compound clusters in the form of a rod-like structure before calcination; the Cu–Zn compound clusters become needle-like crystals over Al_2O_3 after calcination. The distribution of Cu–Zn compound clusters is inconsistent over the Al_2O_3 surface for both CZ and CZNa catalysts. Figure 5c shows good dispersion of Cu–Zn compound clusters over the surface of Al_2O_3 . After calcination, the Cu–Zn compound clusters were separated into small Cu–Zn compound clusters distributed all over the Al_2O_3 surface.

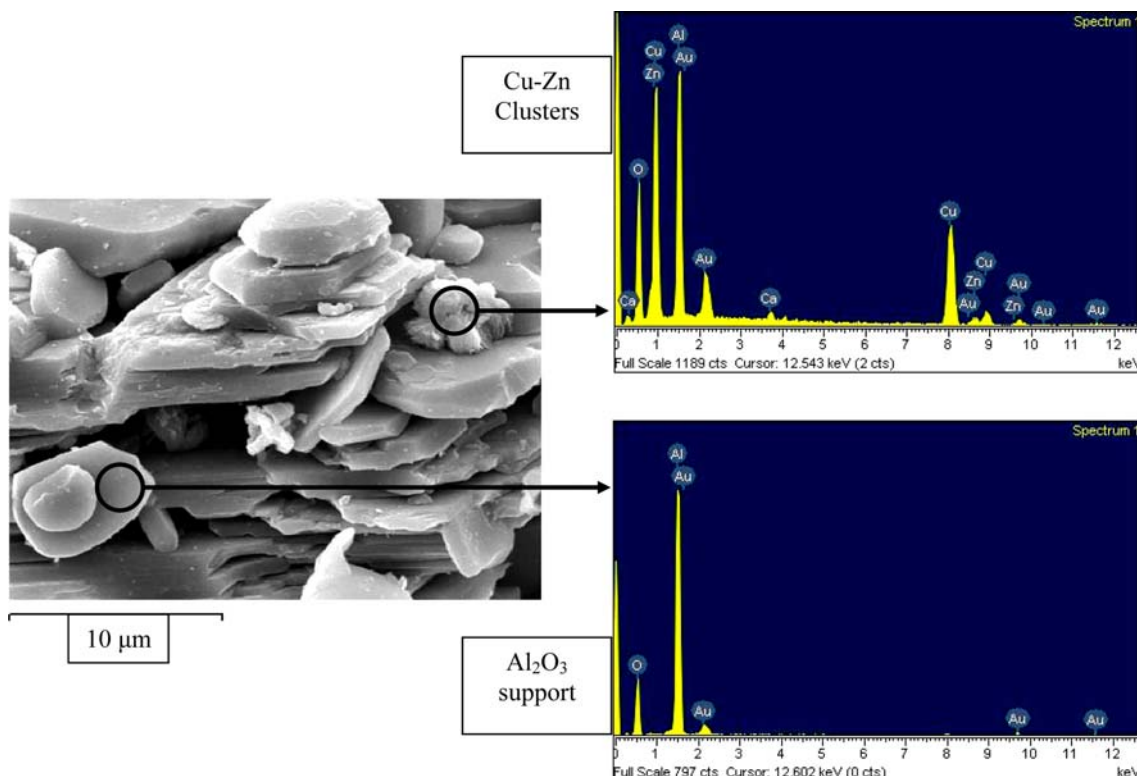


Fig. 1 SEM image and EDS profiles of catalyst formed from impregnated Cu–Zn without urea over Al_2O_3

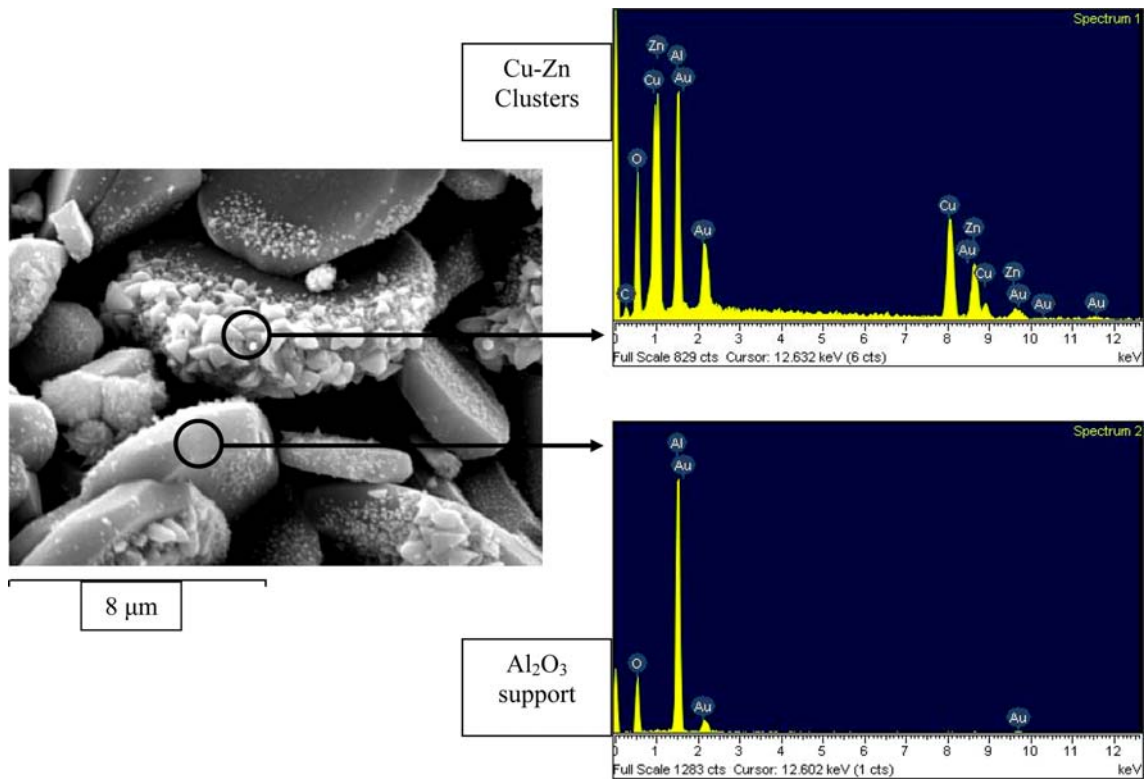


Fig. 2 SEM image and EDS profiles of catalyst formed from impregnated Cu-Zn with urea over Al₂O₃

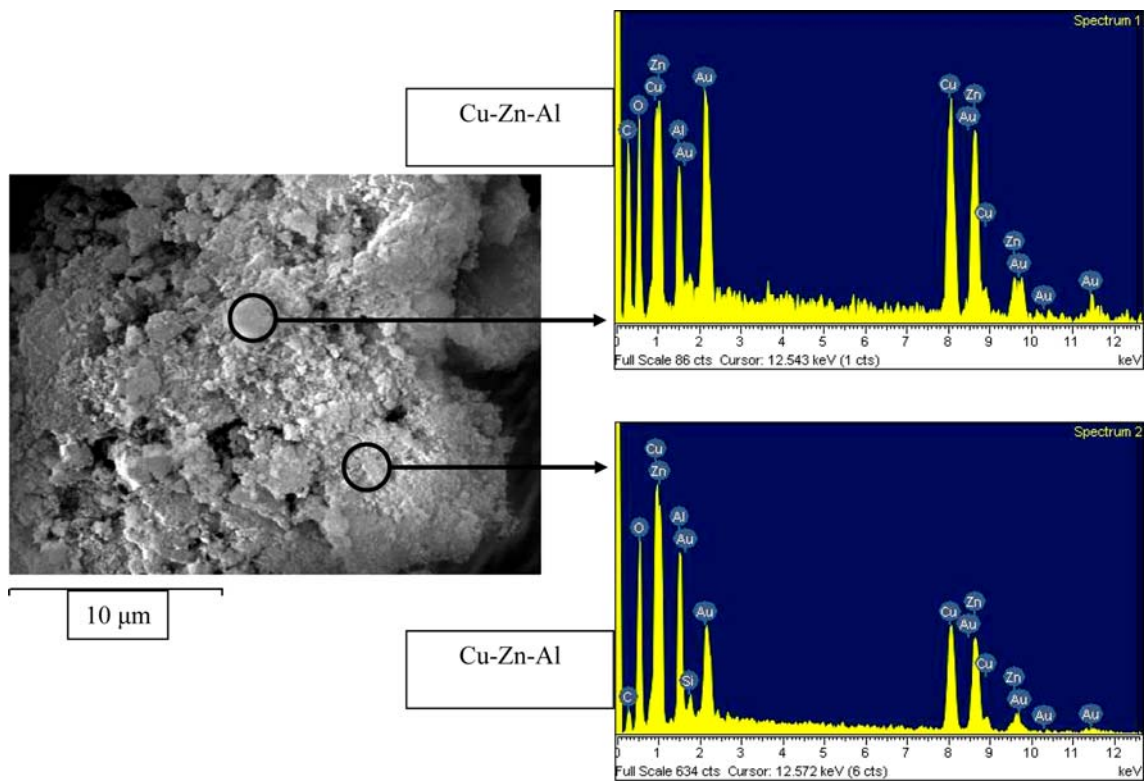


Fig. 3 SEM image and EDS profiles of the commercial catalyst

Fig. 4 SEM images of catalyst formed from impregnated Cu–Zn with and without urea over Al_2O_3 : **a** 20CZ, **b** 20CZU1, and **c** 20CZU2

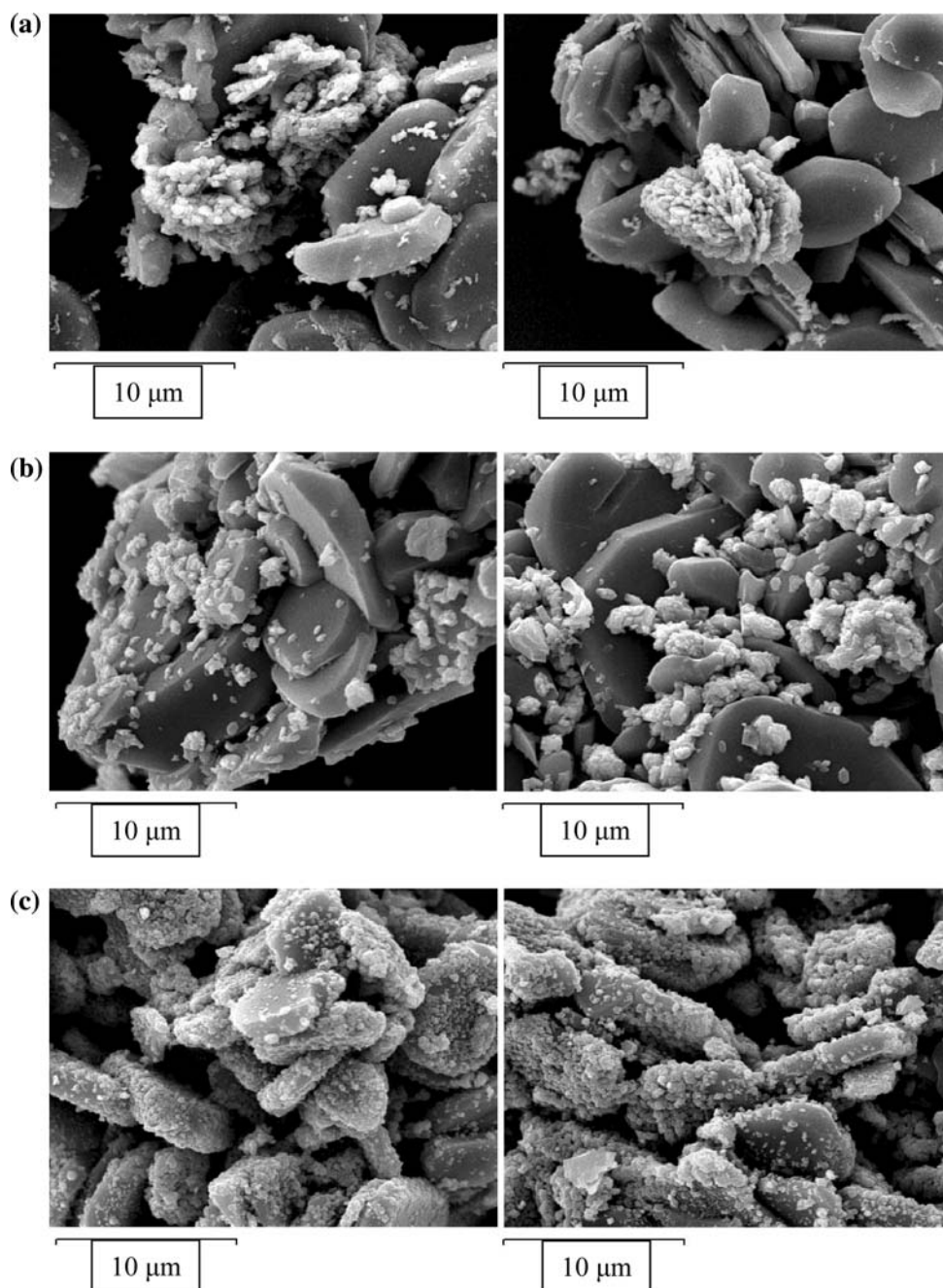
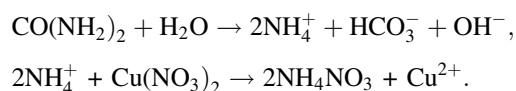
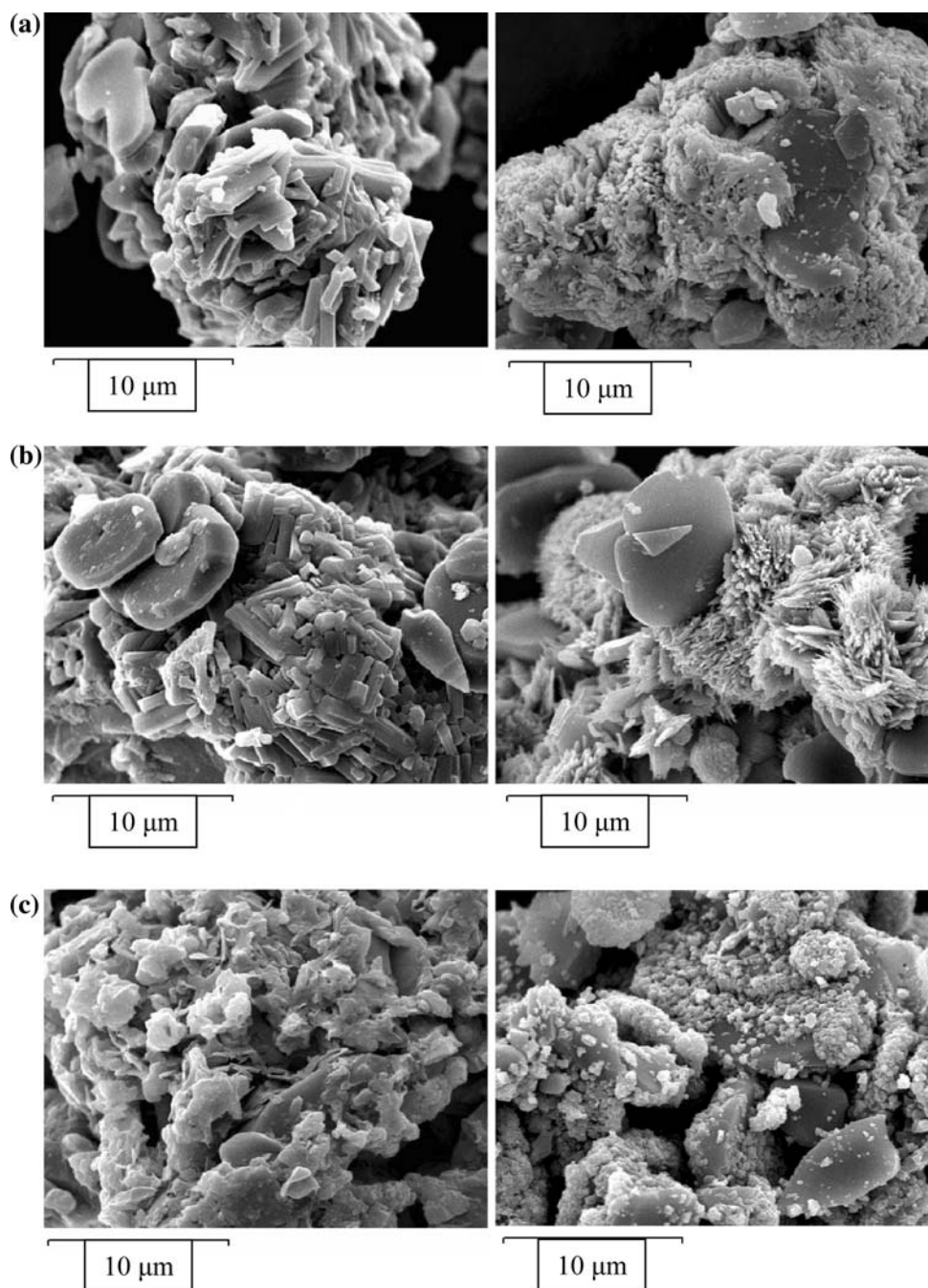


Figure 6 shows X-ray diffractograms of the 20CZ, 20CZU2, and 20CZNa catalysts. The diffractograms of these catalysts exhibit similar patterns. The major phase of these catalysts was composed of copper and zinc nitrate hydroxide. The diffractogram of 20CZU2 exhibits the presence of ammonium nitrate (NH_4NO_3) as a minor phase, which was not found in 20CZ and 20CZNa. The urea that was added to the metal salt solution for impregnation can react with copper nitrate [$\text{Cu}(\text{NO}_3)_2$] and zinc nitrate [$\text{Zn}(\text{NO}_3)_2$] via the following reactions to form NH_4NO_3 :



Based on these reactions, urea can further react with metal nitrates to form NH_4NO_3 , as evidenced in the XRD diffractogram of CZU2. The XRD pattern of NH_4NO_3 disappeared after calcination (Fig. 7). NH_4NO_3 was reported to aid silver, nickel, and ruthenium nanoparticle synthesis in the spray-pyrolysis process. The literature also reports the ability of NH_4NO_3 to undergo explosive

Fig. 5 SEM images of impregnated catalyst before (left) and after calcination (right): **a** 20CZ, **b** 20CZU1, and **c** 20CZU2



decomposition during the calcination process [2, 7, 12]. The NH_4NO_3 produced in the catalysts with the addition of urea can enable size reduction of the Cu–Zn compound clusters and also improve their distribution over the Al_2O_3 surface during calcination.

Figure 7 shows X-ray diffractograms of the impregnated catalysts and the commercial precipitated catalyst. The peaks at $2\theta = 31.8^\circ$, 34° , and 36.2° indicate zinc oxide (zincite, JCPDS no.: 36-1451). Copper oxide (tenorite, JCPDS No.: 45-0937) peaks were observed at $2\theta = 35.8^\circ$ and 38.8° . The diffractogram of the impregnated catalysts

(CZ, CZU, and CZNa) exhibits a similar pattern to the commercial catalyst. The data confirm that the Cu–Zn compounds of the catalysts in this study are the same phases as in the commercial catalyst. Table 2 presents the estimated crystal size of CuO for the catalysts. The data show that a higher amount of urea used in the catalyst impregnation process yields a smaller crystal size of CuO for catalysts with both 10 and 20 wt% metal loading. The crystal size of CuO on the Cu–Zn catalyst using NaOH (CZNa) is not significantly lower compared with on the Cu–Zn catalyst without NaOH (CZ). Therefore, the

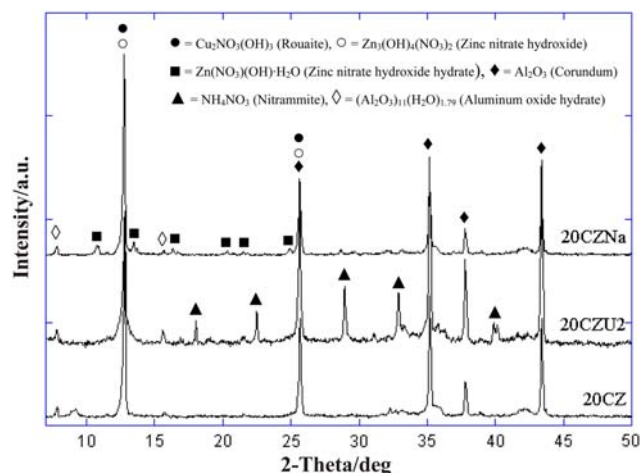


Fig. 6 X-ray diffractograms of impregnated catalysts before calcination

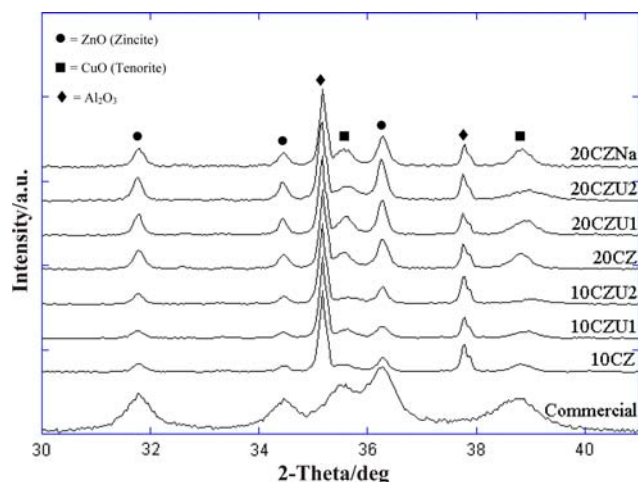


Fig. 7 X-ray diffractogram of impregnated catalysts and commercial catalyst

Table 2 Estimated crystal size of CuO

Sample	Estimated crystal size of CuO ^a (nm)
10CZ	28
10CZU1	21
10CZU2	14
20CZ	29
20CZNa	24
20CZU1	22
20CZU2	14
Commercial	10

^a Determined by XRD using the peak at $2\theta = 38.8^\circ$

basicity of the metal salt solution with NaOH in the impregnation process does not significantly affect the size of crystallized CuO. Unlike NaOH, urea can be added to

the metal salt solution not only to reduce the size of the Cu–Zn compound clusters on the catalyst but also to reduce the crystal size of CuO.

Conclusions

This study shows that urea can improve the activity of Cu–Zn catalysts for the methanol steam reforming reaction. Impregnated Cu–Zn catalysts using urea (CZU2) with lower metal loading can exhibit comparable hydrogen yield to that of the commercial precipitated catalyst with higher metal loading. The catalysts were investigated in order to study the role of urea. SEM–EDS images showed that Cu and Zn are deposited as clusters over Al₂O₃. Images also show that use of urea can reduce the size of the Cu–Zn compound clusters and improve their dispersion over the Al₂O₃ surface. This phenomenon can be explained by the presence of NH₄NO₃ produced by the reaction of urea and metal salt solution, as evidenced in the XRD pattern of the catalyst before calcination. NH₄NO₃ can reduce the size of Cu–Zn compound clusters over Al₂O₃ and also the crystal size of CuO, as determined by XRD. Good dispersion of small Cu–Zn compound clusters over Al₂O₃ results in higher activity for hydrogen production. This study shows that the methanol reforming reaction can be carried out at temperatures as low as 453 K, which can save a lot of energy expenditure.

The production cost of the catalysts can also be lower due to the ease of the preparation process and the lower metal loading compared with commercial catalyst. The choice of an appropriate Cu–Zn metal loading with the addition of urea during impregnation on a high-surface-area support can enhance the reaction activity and lower the operating temperature. The results of this study lead us further towards the development of an effective catalyst for hydrogen production by the methanol reforming process.

Experimental

Catalyst preparation

Cu–Zn-based catalysts over Al₂O₃ were prepared by incipient wetness impregnation. Three types of catalysts were made by using three different Cu–Zn salt aqueous solutions: the metal solution with urea (CZU), without urea (CZ), and with NaOH (CZNa). The catalysts prepared without urea (CZ) were synthesized by impregnating aqueous solution of Cu(NO₃)₂·3H₂O (99%, Fluka) and Zn(NO₃)₂·6H₂O (99%, Fluka) over Al₂O₃ (98%, Riedel-de Haën). The activity of Cu–Zn catalyst using NaOH instead of urea was also tested in order to study the effect of the

Table 3 Compositions of Cu–Zn catalysts for methanol reforming

Catalyst	Composition (Cu/Zn/Al ₂ O ₃ (%wt))	Urea (mol/mol Cu)
10CZ	5/5/90	0
10CZU1	5/5/90	1
10CZU2	5/5/90	2
20CZ	10/10/80	0
20CZU1	10/10/80	1
20CZU2	10/10/80	2
20CZNa ^a	10/10/80	0
Commercial	40/30/30	0

^a The pH of the metal salt solution was adjusted by using NaOH to be equivalent to that of the metal salt–urea solution

basicity of the metal salt solution on the activity of the catalyst. The catalyst prepared with NaOH (CZNa) was synthesized by impregnating aqueous solution of Cu(NO₃)₂·3H₂O and Zn(NO₃)₂·6H₂O with the addition of NaOH (≥98%, Sigma-Aldrich) over Al₂O₃. The pH of the metal salt solution was adjusted using NaOH to be equivalent to that of the metal salt–urea solution. The catalysts prepared with urea (CZU) were synthesized by impregnating aqueous solution of Cu(NO₃)₂·3H₂O and Zn(NO₃)₂·6H₂O with the addition of urea (99%, Carlo Erba) over Al₂O₃. Two molar ratios (1 mol urea, CZU1; 2 mol urea, CZU2) were prepared to study the effect of the amount of urea in catalyst preparation on catalyst activity. Impregnated samples were dried in air at 373 K for 12 h and then calcined at 573 K for 3 h. The commercial catalyst used for comparison was Cu/Zn/Al₂O₃ (Süd-Chemie AG, München, Germany) prepared by precipitation method. The compositions of the catalysts in this study and their abbreviations are shown in Table 3.

Methanol reforming reaction in tubular reactor

The methanol steam reforming reaction for hydrogen production was studied using the prepared catalysts in a stainless-steel tubular reactor with inside diameter of 1 cm. Two grams of catalyst was packed between quartz wool in the reactor. The catalyst was reduced with 30 cm³/min 10% H₂:N₂ balanced at 453 K for 1 h prior to the methanol reforming reaction test. The reactor was flushed with 30 cm³/min N₂ flow at 453 K for 30 min to remove adsorbed hydrogen from the reduction process. The mixture of methanol and aqueous solution was loaded into a saturator which was heated to 333 K. The composition of methanol and water in the liquid phase was 0.125:0.875 molar ratio. The composition of solutions was calculated by the Aspen Plus simulation program (Aspen Technology Inc., Burlington, MA, USA) to ensure that the composition

of the mixture in the vapor phase was a 1:1 molar ratio at the outlet from the saturator. The vapor of the mixture within the saturator was carried by 20 cm³/min N₂, and sent into the reactor at 453 K and 523 K in a continuous system. The time spent in the packed bed reactor in the continuous system was about 6 s. The product was collected and the hydrogen production was determined by gas chromatograph (GC).

Analysis section

A Perkin Elmer (Waltham, Mass., USA) Autosystem XL gas chromatograph (GC) with Porapak Q column (Supleco, Bellefonte, PA, USA) coupled with a thermal conductivity detector (TCD) was used to determine the amount of hydrogen production. The GC was linked to a computer for automatic determination of peak areas, which could be converted to concentration.

Morphology of the catalysts was inspected by scanning electron microscope (SEM, JEOL JSM-5410; Jeol Inc., Tokyo, Japan). The elemental composition of the catalyst surface was determined by energy-dispersive spectrometry (EDS, Oxford; Oxford Instruments, Oxfordshire, UK) in the SEM.

Catalysts were characterized by the X-ray diffraction technique (XRD, JEOL JDX-3530; Jeol Inc., Tokyo, Japan) using Cu K_{α1} radiation, 2θ = 30–41°, 0.04° step size, 1 s step time. JADE software (Jade Software Corporation Ltd., Christchurch, New Zealand) was used to determine the crystal size of CuO by using the broadening of the peak at 2θ = 38.8°. JADE software was also used to identify phases of the catalysts before and after calcination with reference to the X-ray diffractogram database of the International Centre for Diffraction Data (Newtown Square, PA, USA).

Acknowledgments The authors gratefully acknowledge Dr. Sumritra Charojrochkul from the National Metal and Materials Technology Center Thailand for providing experimental facilities. We also thank Dr. Paul Jerus for commercial catalyst and Mr. Paul Vincent Neilson for English proof-reading. Finally, we would like to thank the Thailand Research Fund (TRF) for financial support (grant MRG4780120).

References

1. Alessandra FL, Elisabete MA (2006) *J Power Sources* 159:667
2. Balcerowiak W, Perkowski I (1987) *J Therm Anal* 32:1777
3. Basile A, Parmaliana A, Tosti S, Iulianelli A, Gallucci F, Espro C, Spooen J (2008) *Catal Today* 137:17
4. Campos Skrobot FC, Rizzo Domingues RCP, Fernandes Machado NRC, Cantão MP (2008) *J Power Sources* 183:713
5. Costantino U, Marmottini F, Sisani M, Montanari T, Ramis G, Busca G, Turco M, Bagnasco G (2005) *Solid State Ionics* 176:2917

6. Koga H, Fukahori S, Kitaoka T, Tomoda A, Suzuki R, Wariishi H (2006) *Appl Catal A* 309:263
7. Morozov IV, Fedorova AA, Knotko AV, Valedinskaja OR, Kemnitz E (2004) *Mendeleev Commun* 14:138
8. Murcia-Mascaros S, Navarro RM, Gomez-Sainero L, Costantino U, Nocchetti M, Fierro JLG (2001) *J Catal* 198:338
9. Papavasiliou J, Avgouropoulos G, Ioannides T (2007) *Appl Catal B* 69:226
10. Patel S, Pant KK (2006) *J Power Sources* 159:139
11. Patel S, Pant KK (2007) *Chem Eng Sci* 62:5436
12. Pingali KC, Deng S, Rockstraw DA (2008) *Res Lett Nanotechnol*. doi:[10.1155/2008/756843](https://doi.org/10.1155/2008/756843)
13. Shishido T, Yamamoto Y, Morioka H, Takaki K, Takehira K (2004) *Appl Catal A* 263:249
14. Shishido T, Yamamoto Y, Morioka H, Takehira K (2007) *J Mol Catal A: Chem* 268:185
15. Turco M, Bagnasco G, Costantino U, Marmottini F, Montanari T, Ramis G, Busca G (2004) *J Catal* 228:43
16. Turco M, Bagnasco G, Costantino U, Marmottini F, Montanari T, Ramis G, Busca G (2004) *J Catal* 228:56
17. Xu J, Yeung CMY, Ni J, Meunier F, Acerbi N, Fowles M, Tsang SC (2008) *Appl Catal A* 345:119
18. Yao CZ, Wang LC, Liu YM, Wu GS, Cao Y, Dai WL, He HY, Fan KN (2006) *Appl Catal A* 297:151
19. Zhou L, Guo Y, Zhang Q, Yagi M, Hatakeyama J, Li H, Chen J, Sakurai M, Kameyama H (2008) *Appl Catal A* 347:200